Simulating clinical studies of the glucoregulatory system: in vivo meets in silico

Wendt, Sabrina Lyngbye; Ranjan, Ajenthen; Møller, Jan Kloppenborg; Boye Knudsen, Carsten; Holst, Jens Juul; Madsbad, Sten; Madsen, Henrik; Nørgaard, Kirsten; Jørgensen, John Bagterp

Publication date:
2017

Document Version
Publisher's PDF, also known as Version of record

Simulating clinical studies of the glucoregulatory system: *in vivo* meets *in silico*

Sabrina Lyngbye Wendt*[1,2], Ajenthen Ranjan[3,4], Jan Kloppenborg Møller[2], Carsten Boye Knudsen[1], Jens Juul Holst[5], Sten Madsbad[3,5], Henrik Madsen[2], Kirsten Nørgaard[3], and John Bagterp Jørgensen[2]

[1]Department of Bioanalysis and Pharmacokinetics, Zealand Pharma, Glostrup, Denmark
[2]Department of Applied Mathematics and Computer Science, Technical University of Denmark, Kongens Lyngby, Denmark
[3]Department of Endocrinology, Hvidovre University Hospital, Hvidovre, Denmark
[4]Danish Diabetes Academy, Odense, Denmark
[5]Faculty of Health and Medical Sciences, University of Copenhagen, Copenhagen, Denmark

Version 1
January, 2017

DTU Compute Technical Report-2017-1. ISSN: 1601-2321.
* Email: slw@zealandpharma.com or slwe@dtu.dk

Abstract: In this report we use a validated model of the glucoregulatory system including effects of insulin and glucagon for simulation studies in seven type 1 diabetes patients. Using simulations, we replicate the results from a clinical study investigating the effect of micro-doses of glucagon on glucose metabolism at varying ambient insulin levels. The report compares *in vivo* and *in silico* results head-to-head, and discusses similarities and differences. We design and simulate simple studies to emphasize the implications of some glucoregulatory dynamics which are ignored in most previous clinical studies: the effect of discontinuing insulin and glucose infusions prior to glucagon administration, the delayed effect of insulin, timing of data sampling, and carry-over effects from multiple subcutaneous doses of glucagon. We also use simulations to discuss two hypotheses of how insulin and glucagon might interact in influencing the glucose response. Following the simulations we propose a study design that potentially could explore if the hypotheses are true or false.
Keywords: Glucagon, Glucoregulatory system, Glucose, Insulin, Simulation

Preface

This technical report aims to discuss how to conduct clinical studies seeking to elucidate the dynamics in the glucoregulatory system with focus on glucagon. The discussion is based on published clinical data and simulation experiments using a newly validated glucose-insulin-glucagon model [1].
Simulation models describing insulin and glucagon pharmacokinetics and glucose pharmacodynamics are presented in the first section along with subject specific model parameters and their interpretations.
Second section presents an *in silico* replication of the highly cited study by El Youssef *et al.* from 2014 with the title "Quantification of the Glycemic Response to Microdoses of Subcutaneous Glucagon at Varying Insulin Levels" [2]. All results and graphs of the original paper are replicated using simulations. We present a comparison between the *in silico* and the *in vivo* results.
Third section describes a simulation study exploiting the ability of computer simulations to conduct infinite number of trials thereby creating smooth dose-response curves for glucagon at varying insulin levels with glucagon doses ranging from 1 μg to 10 mg. This section also discusses two possible hypotheses describing the interaction between insulin and glucagon, and suggests a study design that could evaluate the hypotheses.
Based on simulation studies and published clinical studies, fourth section discusses pearls and pitfalls for conducting clinical studies of the glucoregulatory system with focus on trials including glucagon. This last section contains a thorough discussion of the importance of clamp study designs and limitations to identify dynamics in data.

Abbreviations

AUC	area under the curve
AUC_{60}	AUC over 60 minutes
EGP	endogenous glucose production
HbA_{1c}	glycated hemoglobin A1c
IIR	insulin infusion rate
IQR	inter quartile range
MPC	model predictive control
PD	pharmacodynamic
PID	proportional integral derivative
PK	pharmacokinetic
SD	standard deviation
SS	steady state
SC	subcutaneous
Tmax	time to maximum concentration
T1D	type 1 diabetes

Contents

1 Simulation Model

The simulation models in this section including equations and parameter values were published by Wendt *et al.* [1]. For details on the model validation and parameter estimation the reader is kindly referred to the original publication. This section serves as a summary of the model providing the information necessary to use the model for simulations.

1.1 Insulin Pharmacokinetics Model

The insulin pharmacokinetics (PK) model is adopted from Haidar *et al.* [3] and described by equations (1)-(3).

$$\frac{\mathrm{d}X_1(t)}{\mathrm{d}t} = u_I(t) - \frac{X_1(t)}{t_{max}} \tag{1}$$

$$\frac{\mathrm{d}X_2(t)}{\mathrm{d}t} = \frac{X_1(t)}{t_{max}} - \frac{X_2(t)}{t_{max}} \tag{2}$$

$$I(t) = \frac{1}{t_{max}} \frac{X_2(t)}{W \cdot Cl_{F,I}} 10^6 + I_b \tag{3}$$

The steady state conditions of the system are both states, X_1 and X_2, equal to zero. The interpretations of the insulin PK model variables are listed in Table 1. Individual model parameter values are presented in Section 1.4.

Table 1: Interpretation of insulin PK model states, input, output and parameters.

Class	Variable	Unit	Interpretation
States	$X_1(t)$	U	insulin mass due to SC doing, in SC tissue
	$X_2(t)$	U	insulin mass due to SC dosing, in serum
Input	$u_I(t)$	U/min	insulin dose
Output	$I(t)$	mU/L	insulin concentration in serum
Parameters	I_b	mU/L	steady state insulin concentration
	t_{max}	min	time to maximum serum concentration
	W	kg	body weight
	$Cl_{F,I}$	mL/kg/min	apparent insulin clearance

1.2 Glucagon Pharmacokinetics Model

The glucagon PK model is adopted from Wendt *et al.* [4] and described by equations (4)-(6).

$$\frac{\mathrm{d}Z_1(t)}{\mathrm{d}t} = u_C(t) - k_1 Z_1(t) \tag{4}$$

$$\frac{\mathrm{d}Z_2(t)}{\mathrm{d}t} = k_1 Z_1(t) - k_2 Z_2(t) \tag{5}$$

$$C(t) = \frac{k_2 Z_2(t)}{W \cdot Cl_{F,C}} + C_b \tag{6}$$

The steady state conditions of the system are both states, Z_1 and Z_2, equal to zero. Table 2 lists the interpretations of glucagon PK model variables. Individual model parameter values are presented in Section 1.4.

Table 2: Interpretation of glucagon PK model states, input, output and parameters.

Class	Variable	Unit	Interpretation
States	$Z_1(t)$	pg	glucagon mass due to SC dosing, in SC tissue
	$Z_2(t)$	pg	glucagon mass due to SC dosing, in plasma
Input	$u_C(t)$	pg/min	glucagon dose
Output	$C(t)$	pg/mL	glucagon concentration in plasma
Parameters	C_b	pg/mL	steady state glucagon concentration
	k_1	min^{-1}	absorption rate constant
	k_2	min^{-1}	elimination rate constant
	W	kg	body weight
	$Cl_{F,C}$	mL/kg/min	apparent glucagon clearance

1.3 Glucose Pharmacodynamics Model

The glucose pharmacodynamics (PD) model was first developed using preclinical data from healthy dogs [4] and then tested with data from healthy humans [5]. Finally, the PD model was validated for simulations in seven type 1 diabetes patients [1]. The model structure is described by equations (7)-(13).

$$\frac{\mathrm{d}Q_1(t)}{\mathrm{d}t} = -F_{01} - F_R - S_T x_1(t) Q_1(t) + k_{12} Q_2(t) + G_{GG}(t) + G_{GNG} \quad (7)$$

$$\frac{\mathrm{d}Q_2(t)}{\mathrm{d}t} = S_T x_1(t) Q_1(t) - [k_{12} + S_D x_2(t)] Q_2(t) \quad (8)$$

$$G_{GG}(t) = \frac{1 - S_E x_3(t)}{1 - S_E \mathrm{I}_b} \cdot \left((E_{max} - G_{GNG}) \frac{C(t)}{C_{E50} + C(t)} \right) \quad (9)$$

$$G(t) = \frac{Q_1(t)}{\mathrm{V}} \quad (10)$$

$$\frac{\mathrm{d}x_1(t)}{\mathrm{d}t} = k_{a1}[I(t) - x_1(t)] \quad (11)$$

$$\frac{\mathrm{d}x_2(t)}{\mathrm{d}t} = k_{a2}[I(t) - x_2(t)] \quad (12)$$

$$\frac{\mathrm{d}x_3(t)}{\mathrm{d}t} = k_{a3}[I(t) - x_3(t)] \quad (13)$$

In equation (9), $1 - S_E x_3(t)$ is always greater than or equal to zero. Interpretations of PD model states, inputs, outputs and parameters are listed in Table 3. Subject specific model parameters are presented in Section 1.4. The steady state conditions of the model are listed in equations (14)-(18).

$$Q_{1,SS} = G_{SS} \cdot V \quad (14)$$

$$Q_{2,SS} = Q_{1,SS} \frac{x_{1,SS}}{x_{2,SS} + k_{12}} \quad (15)$$

$$x_{1,SS} = I_b \quad (16)$$

$$x_{2,SS} = I_b \quad (17)$$

$$x_{3,SS} = I_b \quad (18)$$

1.4 Model Parameters

The majority of PK and PD model parameters are subject specific and listed in Table 4. A few parameters are fixed for all subjects including the rate of gluconeogenesis, G_{GNG}, at 6 μmol/kg/min [6], and the glucose volume of distribution, V, at 160 mL/kg [7]. The renal clearance of glucose is zero unless the plasma glucose concentration exceeds 9 mmol/L in which case it is calculated as $0.003 \cdot (G - 9) \cdot V$ [8]. Similarly, the insulin independent glucose flux is calculated as $F_{01} \cdot G/4.5$ when the plasma glucose concentration falls below 4.5 mmol/L [8].
The glucose PD model was validated using leave-one-out cross-validation in seven out of eight type 1 diabetes patients. The model parameters of patient 8 are reported although the model could not be validated in this subject. Therefore, simulations in the following chapters are carried out using only subjects 1-7.

Table 3: Interpretation of glucose PD model states, input, output and parameters.

Class	Variable	Unit	Interpretation
States	$Q_1(t)$	μmol/kg	glucose mass per W in the accessible compartment
	$Q_2(t)$	μmol/kg	glucose mass per W in the non-accessible compartment
	$x_1(t)$	mU/L	remote effects of insulin on glucose transport
	$x_2(t)$	mU/L	remote effects of insulin on glucose disposal
	$x_3(t)$	mU/L	remote effects of insulin on glycogenolysis
Inputs	$I(t)$	mU/L	insulin concentration in serum
	$C(t)$	pg/mL	glucagon concentration in plasma
Outputs	$G(t)$	mmol/L	glucose concentration in plasma
	$G_{GG}(t)$	μmol/kg/min	glucose production due to glycogenolysis
Parameters	G_{GNG}	μmol/kg/min	glucose production due to gluconeogenesis
	C_{E50}	pg/mL	glucagon concentration yielding half of maximum EGP
	E_{max}	μmol/kg/min	maximum EGP at basal insulin concentration
	F_{01}	μmol/kg/min	insulin independent glucose flux
	F_R	μmol/kg/min	renal glucose clearance
	$k_{12} \cdot 10^{-4}$	min^{-1}	transfer rate constant from Q_2 to Q_1
	$k_{a1} \cdot 10^{-4}$	min^{-1}	insulin deactivation rate constant
	$k_{a2} \cdot 10^{-4}$	min^{-1}	insulin deactivation rate constant
	$k_{a3} \cdot 10^{-4}$	min^{-1}	insulin deactivation rate constant
	$S_D \cdot 10^{-4}$	min^{-1}/(mU/L)	insulin sensitivity of glucose disposal
	$S_E \cdot 10^{-4}$	$(\text{mU/L})^{-1}$	insulin sensitivity of glycogenolysis
	$S_T \cdot 10^{-4}$	min^{-1}/(mU/L)	insulin sensitivity of glucose transport
	V	mL/kg	glucose volume of distribution

Table 4: Subject specific PK/PD model parameters used for simulations.

Parameter		Patient							
		1	2	3	4	5	6	7	8
W	[kg]	54	50	81	69	87	72	73	59
I_b	[mU/L]	7.3	10.6	11.7	8.7	6.6	5.5	19.7	7.4
t_{max}	[min]	57.6	57.3	40.8	67.9	48.5	46.5	68.5	55.4
$Cl_{F,I}$	[mL/kg/min]	18.9	18.5	14.8	17.4	17.3	24.6	23.7	26.8
C_b	[pg/mL]	10.7	7.6	7.6	10.9	8.7	8.9	11.6	19.0
k_1	[min^{-1}]	0.042	0.056	0.022	0.058	0.038	0.035	0.035	0.052
k_2	[min^{-1}]	0.14	0.26	0.10	0.058	0.19	0.28	0.25	0.090
$Cl_{F,C}$	[mL/kg/min]	94	106	114	159	200	125	136	91
C_{E50}	[pg/mL]	436	405	401	285	339	424	141	307
E_{max}	[μmol/kg/min]	56.4	67.4	57.4	84.4	65.4	60.1	78.0	75.3
F_{01}	[μmol/kg/min]	14.2	13.8	15.5	12.8	12.0	13.1	14.2	13.4
$k_{12} \cdot 10^{-4}$	[min^{-1}]	244	285	397	213	281	238	358	289
$k_{a1} \cdot 10^{-4}$	[min^{-1}]	16	15	18	18	15	10	49	37
$k_{a2} \cdot 10^{-4}$	[min^{-1}]	522	495	548	437	517	353	624	518
$k_{a3} \cdot 10^{-4}$	[min^{-1}]	215	231	327	68	235	74	178	154
$S_D \cdot 10^{-4}$	[min^{-1}/(mU/L)]	1.5	1.2	1.4	2.0	1.1	2.6	4.4	4.2
$S_E \cdot 10^{-4}$	[$(\text{mU/L})^{-1}$]	155	334	237	415	229	404	140	463
$S_T \cdot 10^{-4}$	[min^{-1}/(mU/L)]	23	19	25	18	31	21	21	29

2 The Study by El Youssef *et al.*

In this section, using simulations we aim to replicate the clinical study by El Youssef *et al.* published in Diabetes Care November 2014 with the title "Quantification of the Glycemic Response to Microdoses of Subcutaneous Glucagon at Varying Insulin Levels" [2].

2.1 Study Design

The study by El Youssef *et al.* [2] included 11 type 1 diabetes (T1D) patients (5 females, age IQR: 36.5-46.0 years, BMI IQR: 23.0-31.1 kg/m^2, HbA$_{1c}$ IQR: 7.0-8.2%). The patients participated in three study days of each 10 hours duration with constant intravenous insulin infusion rate (IIR) of either low, medium or high. Average results during low, medium and high IIR are based on 10, 9, and 10 subjects, respectively. Glucose infusion rates were controlled using a proportional integral derivative (PID) controller aiming at a blood glucose concentration of 85 $\pm$ 20 mg/dL. When blood glucose read below 60 mg/dL the controller regulated the glucose infusion rate every five minutes, otherwise every ten minutes. After an initial two hours run-in period the subjects received the first glucagon bolus. They received the second glucagon bolus after another two hours until a total of four glucagon boluses were delivered and observed for the following two hours. The glucagon boluses were delivered in a pseudo-random order by varying the initial dose, but keeping the order: 25 μg, 75 μg, 125 μg, and 175 μg (25-75-125-175, 75-125-175-25, 125-175-25-75, 175-25-75-125). Each subject received the same pseudo-random order of glucagon boluses during each study day.
The study used regular human insulin (Humulin R, Eli Lilly and Company) and glucagon (GlucaGen, Novo Nordisk).

2.2 Simulation Study Details

In the *in silico* study we used the validated patient specific PK/PD models describing seven T1D patients (4 females, age range: 19-64 years, BMI range: 20.0-25.4 kg/m^2, HbA$_{1c}$ range: 6.1-7.4 %) presented in Section 1 [1]. All virtual subjects participated in experiments with low, medium and high IIRs. We followed the study design of the clinical study described in Section 2.1. We allowed initialization of patients at steady state (SS) at the beginning of the two hours run-in period by solving the patient specific equations for SS.
The insulin and glucagon PK/PD model parameters were based on a study using insulin aspart (NovoRapid, Novo Nordisk) and glucagon (GlucaGen, Novo Nordisk). As the IIRs are constant during the experiment the possible differences in insulin PK between Humulin R and NovoRapid are not confounding the study. Differences in insulin PD effects are relevant, however, we assume that the insulins have identical PD effects.

2.2.1 Determining Infusion Rates

The low and medium IIR were chosen based on individual basal infusion rates and the high IIR was fixed at 0.05 U/kg/h for all subjects. In the clinical study they used either

0.01 U/kg/h or the patient's average daytime basal rate as the lowest IIR, but the latter information was not available in the simulation study. Therefore, the individual low IIR was maximized to either 0.01 U/kg/h or the infusion rate yielding an insulin level equal to one and a half times the fasting serum insulin concentration. The medium IIR was chosen halfway between the low and high IIR.
The SS glucose infusion rate was calculated by solving individual glucoregulatory models at SS given the pre-specified insulin infusion rate.

2.2.2 Proportional Integral Derivative Controller

We implemented a simple proportional integral derivative (PID) controller with clipping to control the blood glucose concentration by adjusting the glucose infusion rate, as listed in equations (19)-(22).

$$e_k = G_{SS} - G_k \tag{19}$$

$$I_k = I_{k-1} + k_i \cdot \Delta t \cdot e_k \tag{20}$$

$$\mathrm{d}e_k = \frac{e_k - e_{k-1}}{\Delta t} \tag{21}$$

$$U_k = \max(0, U_{SS} + k_p \cdot e_k + I_k + k_d \cdot \mathrm{d}e_k) \tag{22}$$

G_{SS} is the glucose concentration at SS (set point of 85 mg/dL), G_k is the k^{th} glucose observation, and e_k is the deviation from set point of the k^{th} observation. I_k is the discretization of the integral of errors until k, calculated as the sum of the previous integral of errors, I_{k-1}, and the current integral of error weighted by k_i. $\mathrm{d}e_k$ is the discretization of the error derivative at k calculated by the backward difference. The updated glucose infusion rate, U_k, is the sum of the SS glucose infusion rate, U_{SS}, the error weighted by k_p, the integral of errors, and the error derivative weighted by k_d, unless the sum is negative, in which case the glucose infusion rate is set to zero. We used k_p = 4, k_i = 1, and k_d = -2.

2.2.3 Calculation of Endogenous Glucose Production

The endogenous glucose production (EGP) due to glucagon was directly calculated using the PD model. EGP was baseline-corrected by subtracting the EGP level at the time of the most recent glucagon dose to avoid carry-over effects from previous glucagon doses or from baseline production maintained by the constant insulin infusion and SS glucagon concentration.

$$EGP_{Corrected}(t) = EGP(t) - EGP(t_{Dose,n}) \quad n = 1, ..., 4 \tag{23}$$

The baseline-corrected EGP can thus become negative when current EGP is less than at the time of the most recent glucagon dose. However, it can not be more negative than the difference between EGP at SS and EGP at the time of the most recent glucagon dose.

2.3 Results and Discussion

2.3.1 Insulin and Glucose Infusion Rates

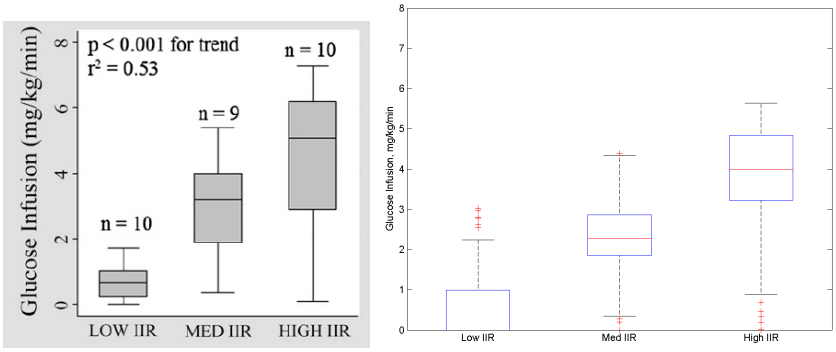

(a) *In vivo* from [2]. (b) *In silico* (n=7).

Figure 1: Box plot of glucose infusion rate (mg/kg/min) across all studies, by insulin infusion group.

Table 5 compares the reported *in vivo* and simulated *in silico* average insulin and glucose infusion rates at low, medium and high IIRs. At a first glance, insulin infusion rates are very similar in the two studies based on averages and medians. However, the virtual study contained one patient (no. 7) having a very high basal IIR yielding a low IIR of 0.042 U/kg/h and a medium IIR of 0.046 U/kg/h. Ultimately, there was little differences between the three IIRs in this subject and therefore only minor differences in responses during the various insulin infusion rates. The high basal IIR indicates that the subject is not very sensitive to insulin and therefore the response to glucagon during the high IIR was little attenuated by the insulin level. No formal test was performed to exclude this subject. However, the low IIR and medium IIR are more than two standard deviations from the mean infusion rates reported *in vivo* which justifies the exclusion of the subject from the analysis of EGP response to glucagon at various insulin levels.

Table 5: Summary of insulin and glucose infusion rates *in vivo* and *in silico*. Infusion rates are reported as mean ± SD and median [IQR]. L = low, M = medium, H = high.

	IIR	*In Vivo*		*In Silico*	
Insulin	L	0.016 ± 0.006	0.014	0.018 ± 0.011	0.014
rate	M	0.032 ± 0.003	0.03	0.034 ± 0.006	0.032
U/kg/h	H	0.05 ± 0.00	0.05	0.05 ± 0.00	0.05
Glucose	L	0.7 ± 0.5	0.6 [0.2-1]	0.5 ± 0.8	0.0 [0.0-1.0]
rate	M	2.9 ± 1.3	3.2 [1.9-4]	2.1 ± 0.9	2.3 [1.9-2.9]
mg/kg/min	H	4.5 ± 2	5.1 [2.9-6.2]	3.8 ± 1.2	4.0 [3.2-4.8]

Summary statistics of glucose infusion rates are similar although the interquartile range

is narrower *in silico* than *in vivo*. This difference is also evident in Figure 1 showing smaller boxes but several outliers *in silico* compared to *in vivo*. Looking at the glucose infusion rates over time in Figure 2b, we observe a difference in the response to glucagon, thus the amount of decrease in glucose infusion rate compared to Figure 2a. Moreover, the glucose infusion rate at SS is slightly lower during medium and high IIRs. To the authors it is not clear how the large decrease in glucose infusion rate during high IIR displayed in Figure 2a relates to the small EGP area under the curve (AUC) displayed in Figure 8a.

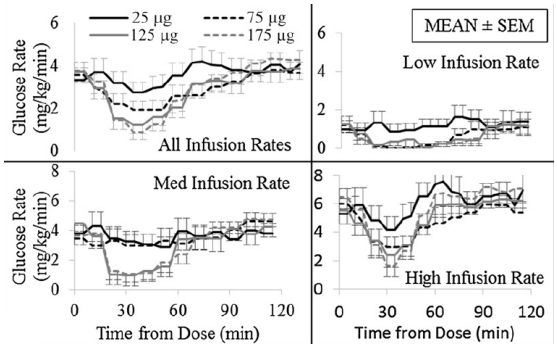

(a) *In vivo* from [2].

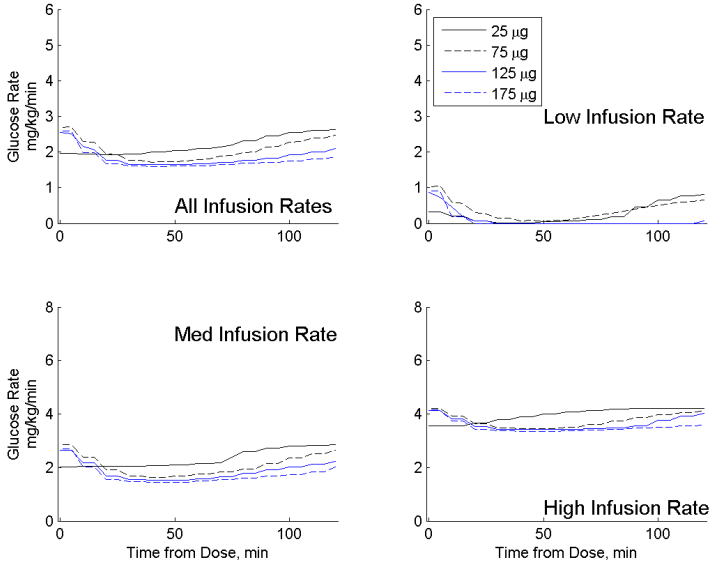

(b) *In silico* (n=7).

Figure 2: Mean glucose infusion (mg/kg/min) over time by insulin infusion rate group and glucagon dose: top left, all insulin infusion rates together; top right, bottom left, and bottom right, low, medium, and high insulin infusion rates, respectively.

2.3.2 Insulin and Glucose Concentrations

Table 6 compares reported and simulated serum insulin concentrations and plasma glucose concentrations after the two hours run-in period. The distribution of serum insulin levels are very similar in the clinical and virtual studies as seen in Figure 3. This confirms that the insulin PK model is applicable despite not being estimated from optimally sampled data as described in [1]. On the contrary, the plasma glucose concentrations differ. The glucose concentration is lower with less variation during the *in silico* experiment especially during low and medium IIR. This is probably due to differences in the PID controller settings achieving better control in the virtual population than in real subjects. Moreover, using the SS equations of the individual subjects we calculated the exact needed glucose infusion rate to counter the IIR. This is unfortunately not possible in real life. The plasma glucose concentration is equally well controlled during the high IIR which is probably due to the attenuated EGP response to glucagon.

Table 6: Serum insulin and plasma glucose concentrations *in vivo* and *in silico*. Concentrations are reported as mean ± SD and median [IQR]. L = low, M = medium, H = high.

	IIR	*In Vivo*		*In Silico*	
Serum	L	17.6 ± 13.0	11.0 [9.7-24.6]	15.0 ± 7.2	13.1 [10.2-17.1]
insulin	M	29.1 ± 8.9	28.1 [25.5-31.5]	29.7 ± 4.8	30.5 [28.0-31.9]
mU/L	H	46.0 ± 12.5	41.7 [37.5-46.8]	44.4 ± 7.8	45.1 [37.4-48.1]
Plasma	L	150.8 ± 68.3		100.5 ± 28.0	
glucose	M	92.9 ± 21.3		83.6 ± 14.6	
mg/dL	H	88.0 ± 16.0		83.4 ± 13.4	

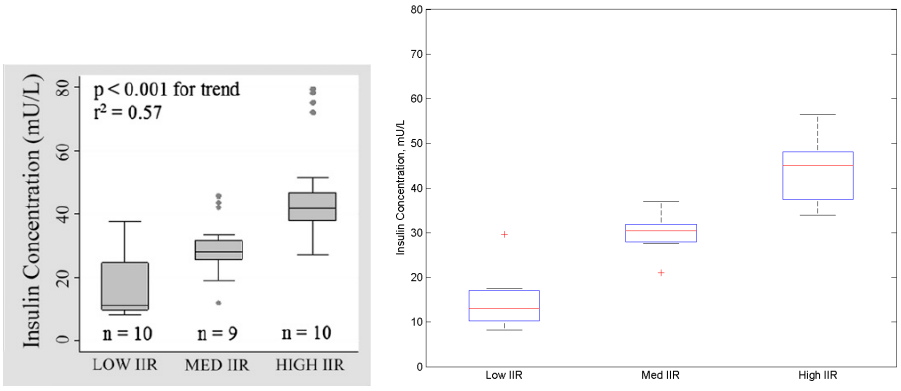

(a) *In vivo* from [2]. (b) *In silico* (n=7).

Figure 3: Box plot of serum insulin levels (mU/L) at low, medium, and high insulin infusion rates.

2.3.3 Glucagon

Table 7 compares time to maximum concentration (Tmax) of glucagon between the clinical and virtual studies stratified by glucagon dose. In both studies, Tmax did not dependent on glucagon dose. We found smaller Tmax with smaller variation *in silico* than *in vivo*. One should keep in mind that blood was only sampled every 10 minutes in the clinical study whereas data used for estimating glucagon PK model parameters for simulations were sampled every 5 minutes. Blood sampling every 10 minutes does not allow for accurate determination of glucagon's Tmax.
Comparisons of glucagon AUCs in Figure 4 and concentration time profiles in Figure 5 to the *in vivo* findings should be made with caution as absolute glucagon concentration highly depends on the assay [9]. Moreover, the *in vivo* study measured glucagon in serum whereas the *in silico* study simulated glucagon in plasma. Overall, *in silico* glucagon levels seem more variable, although with clearly separated average PK profiles for each dose.
Figure 5a and 5b show that the plasma glucagon concentration is still above SS two hours after most glucagon doses. Therefore, repeating glucagon dosing after only two hours will likely introduce some carry-over effects from the previous dose, even when baseline-corrected at the time of dose.

Table 7: Glucagon Tmax.

	Dose	*In Vivo*	*In Silico*
Glucagon Tmax min	25 μg	23.2 $\pm$ 13.5	11.1 $\pm$ 3.5
	75 μg	17.1 $\pm$ 8.1	12.1 $\pm$ 4.3
	125 μg	19.6 $\pm$ 6.1	12.1 $\pm$ 4.3
	175 μg	20 $\pm$ 9.6	12.1 $\pm$ 4.3

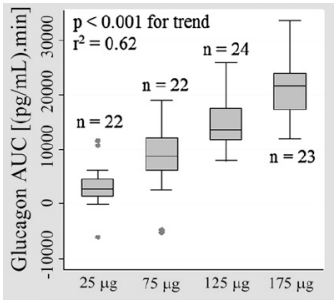

(a) *In vivo* from [2].

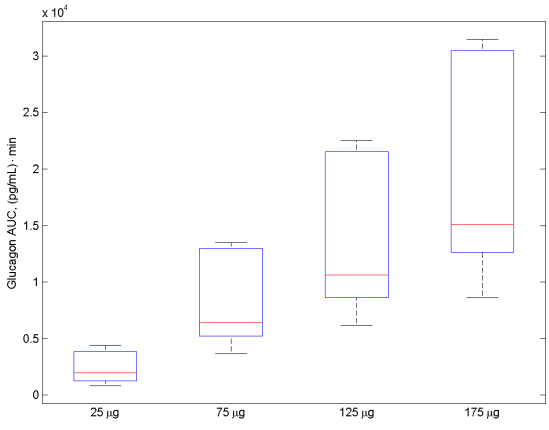

(b) *In silico* (n=21).

Figure 4: Box plot of glucagon plasma level AUC over 60 min, stratified by dose.

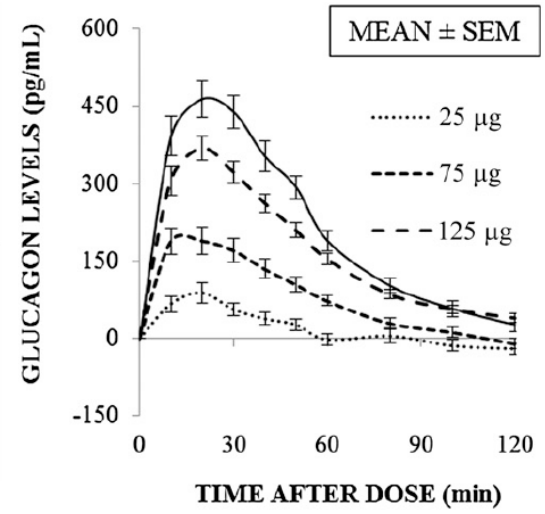

(a) *In vivo* from [2].

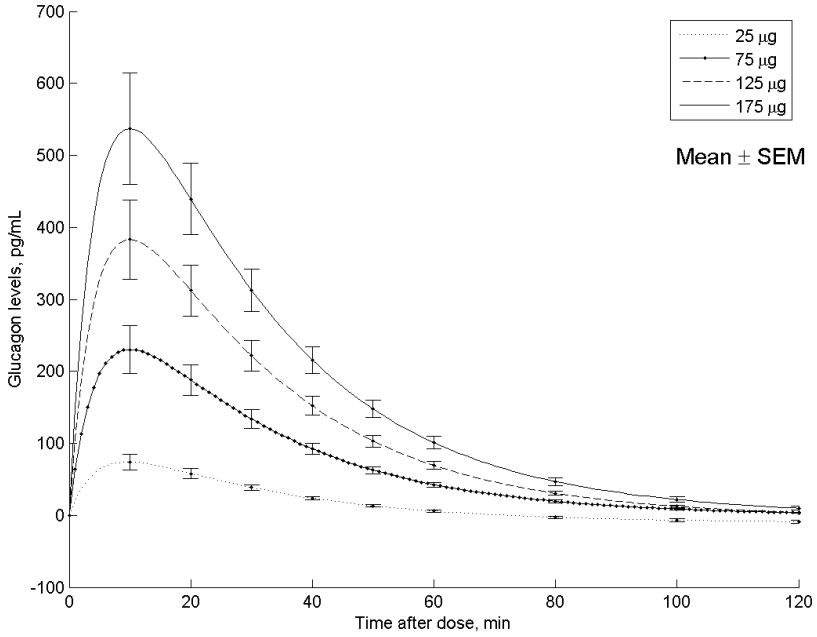

(b) *In silico* (n=21).

Figure 5: Mean incremental change in glucagon plasma levels (baseline corrected at time = 0).

2.3.4 Endogenous Glucose Production

The results in the following section highly depends on the method used for calculating EGP. In the *in vivo* study they derived the EGP from tracer data by fitting a two-compartment model. In the *in silico* study we calculated the EGP directly from the model description.
As mentioned in Section 2.3.1, one patient was considered an outlier because of nearly no difference in IIRs and was excluded from the following analysis of EGP due to glucagon at various insulin levels.

Figure 6b replicates Figure 6a with many similarities but also some differences. Most importantly, the magnitudes of average peak EGP to the four glucagon doses are similar. The EGP increase appears to be more rapid *in silico* than *in vivo* yielding a faster Tmax, which can be partly explained by the faster glucagon Tmax. However, with the sampling of every ten minutes the observed Tmax could be anywhere between 10-30 minutes and the simulated Tmax could be between 0-20 minutes (the average is in fact 12 minutes). If the true Tmax of EGP in response to glucagon is between 10-20 minutes, this fits with both the observed and simulated results.
The *in vivo* estimated EGP returned fast to baseline and after 60 minutes it was below the production before injection of the preceding glucagon bolus. The simulated EGP has slower return to baseline and we only observe slightly negative values after the lowest glucagon dose.

The average EGP over the first 60 minutes is somewhat higher *in silico* than *in vivo* as visualized in Figure 7b compared to Figure 7a. This difference is expected based on the simulated slower return to baseline just described. The simulated averages are however within the standard error of measurement of the observed data.

Perhaps the most interesting graph is Figure 8a which is replicated by simulation in Figure 8b. The averages of the simulated data are different from the observed averages. However, considering the standard error of measurement of both datasets the simulated data is not different from the observed data. The EGP responses to doses of glucagon during medium IIR were very similar to the EGP responses during low IIR in the measured data, whereas we observe a difference between the responses during the two IIRs when simulating the experiments. We also find a small increase in response to increasing glucagon boluses even at high IIR which is not pronounced in the original observed data. In general, the standard error of measurements are smaller *in silico* than *in vivo*.

Figure 9b is a replication of Figure 9a but without extrapolation. The original graph shows the actual data in the dose-range of 25-175 μg glucagon and extrapolates the presumed trends down to 1 μg and up to 10 mg. Note, this is a wild extrapolation with no data to support it. Within the data-range the simulated results match the observed results although the simulated EGP at low IIR tends to be higher than the observed. Having only four points very closely spaced on a log-scale, a single point can largely influence the overall interpretation of the curves.

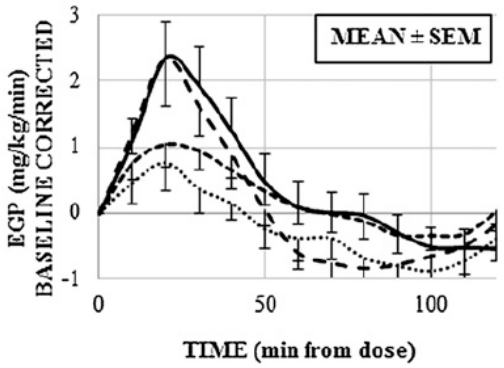

(a) *In vivo* from [2].

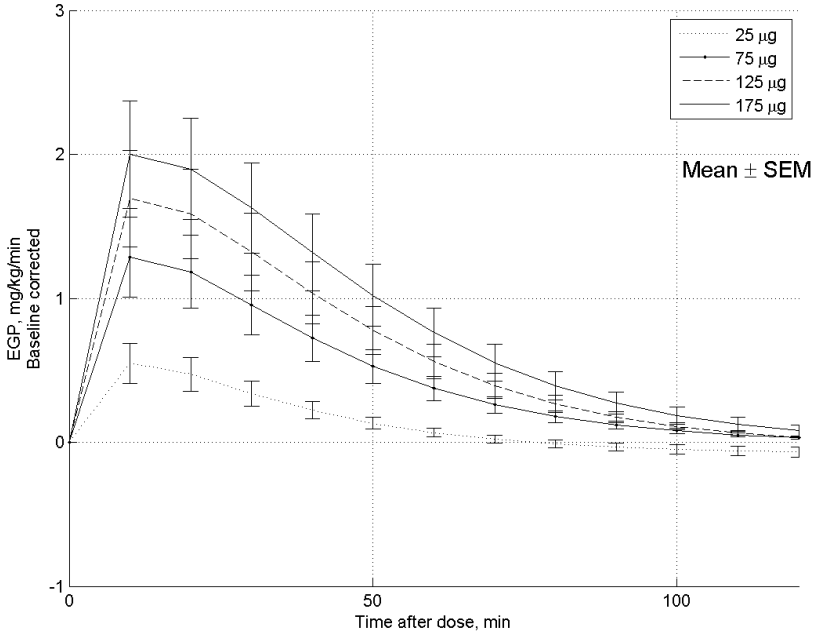

(b) *In silico* (n=6).

Figure 6: Time profiles of calculated EGP by glucagon dose, baseline corrected for EGP at the time of dose.

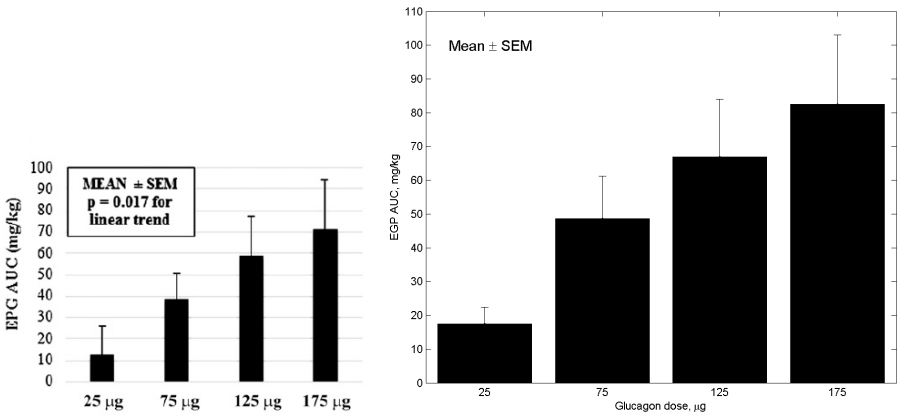

(a) *In vivo* from [2]. (b) *In silico* (n=18).

Figure 7: Mean EGP AUC over 60 min after the dose.

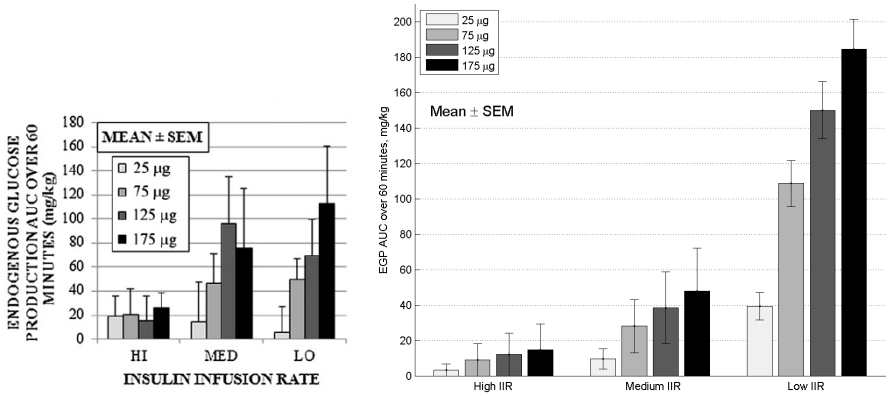

(a) *In vivo* from [2]. (b) *In silico* (n=6).

Figure 8: Mean EGP AUC separated by glucagon dose and insulin infusion rate.

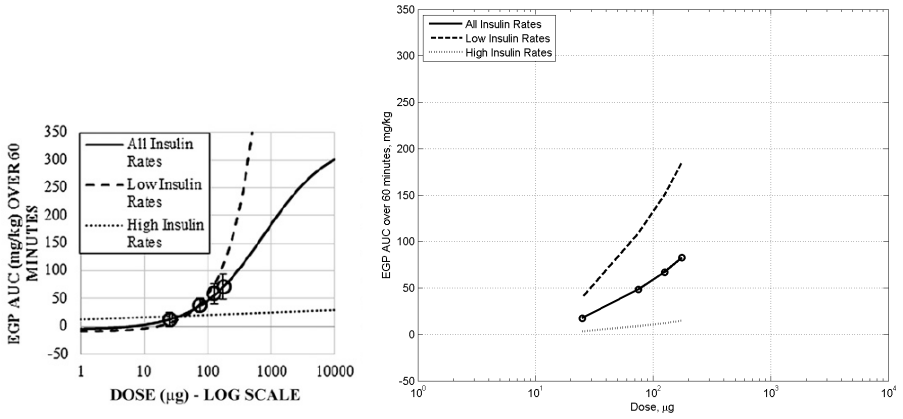

(a) *In vivo* from [2]. (b) *In silico* (n=6 or 18).

Figure 9: Dose-response curve across all doses, and for low and high insulin infusion rate experiments, estimated from simulated data.

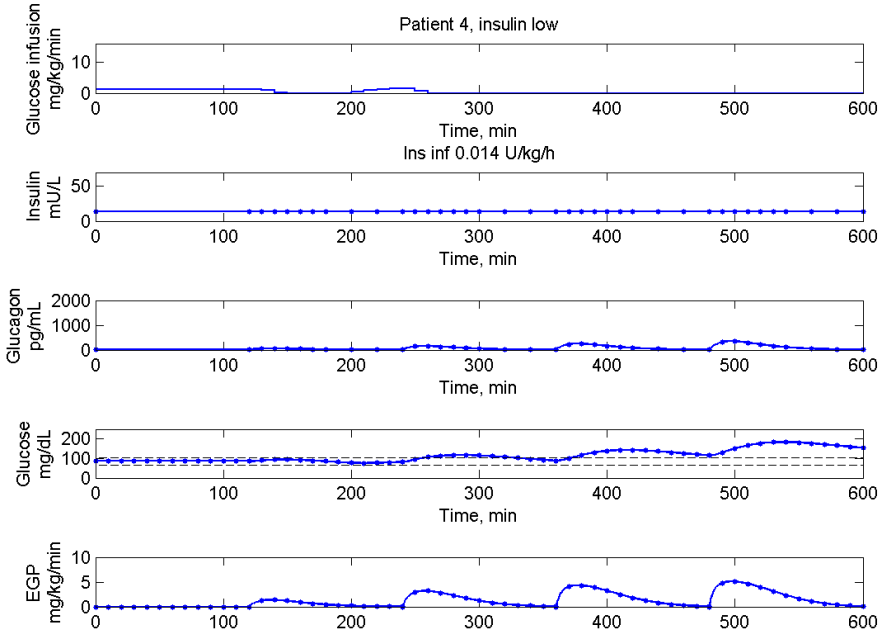

Figure 10: Example of simulated raw data from patient 4 during the low IIR with first bolus being 25 μg. Notice that the blood glucose concentration and glucose infusion rate do not return to SS before the next glucagon bolus is administered.

2.3.5 Examples of Simulated Raw Data

Figures 10 and 11 show examples of raw data from the simulation study. The points mark blood sampling times during the *in vivo* study.

The first figure presents data during low IIR and reveals that the blood glucose level cannot be kept within ± 20 mg/dL of the set point at all times. Especially after the higher doses of glucagon the blood glucose exceeds the upper limit. The graph also reveals that the glucose infusion rate is zero during most of the experiment. The explanation to this observation is that during low IIR the glucose infusion rate needed to maintain SS is equally low and cannot be lowered sufficiently after the glucagon boluses to maintain the blood glucose within the boundaries. Moreover, the plasma glucose concentration and glucose infusion rate do not return to SS before the next glucagon bolus administration.

The second figure shows data during medium IIR where the glucose infusion rate is never zero although decreased in response to glucagon boluses. The blood glucose is mostly kept within the boundaries.

The raw data from the study by El Youssef *et al.* [2] are not available, making it im-

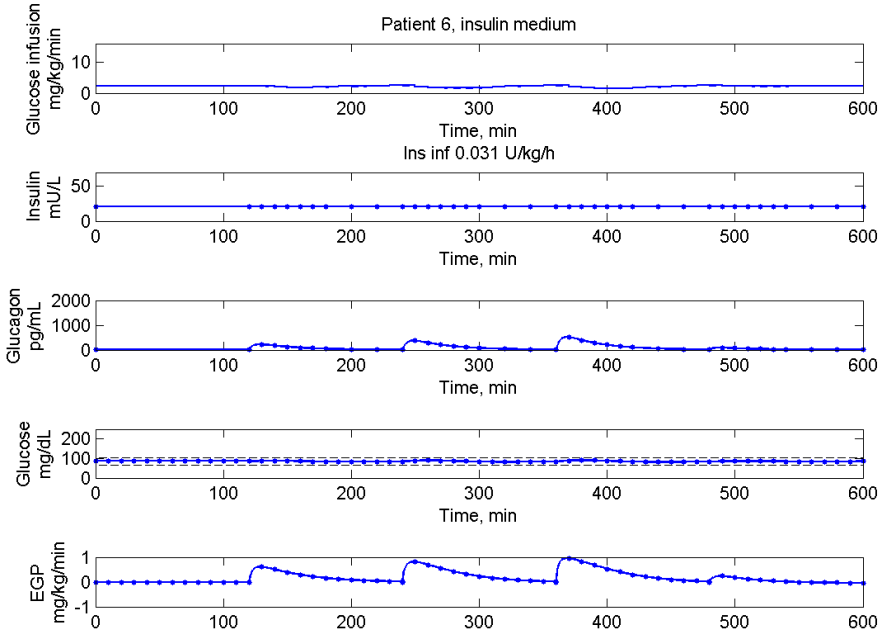

Figure 11: Example of simulated raw data from patient 6 during the medium IIR with first bolus being 75 μg. Notice how the glucose infusion is regulated to control the blood glucose close to the set point.

possible to compare our examples to actual data.

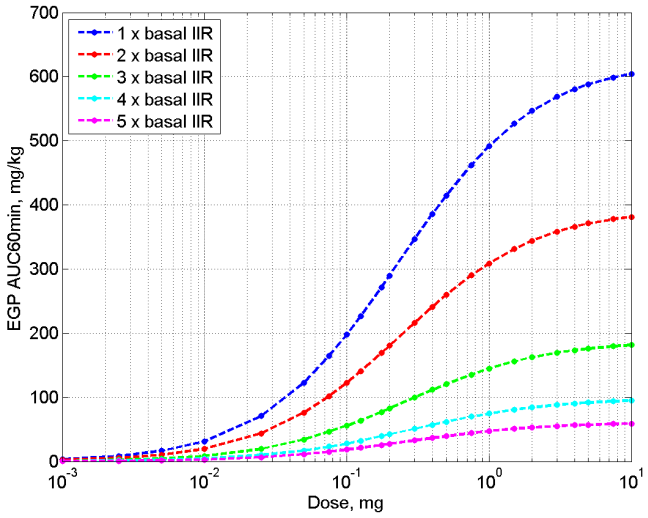

Figure 12: Simulated average of seven T1D patients' dose-response curves of glucagon boluses ranging from 1 μg to 10 mg at various insulin levels expressed as multiples of the basal IIR.

3 Dose-Response Studies

In this section, we demonstrate the advantage of using simulations to conduct large cross-over studies that would not be feasible in real life. Moreover, we use simulations to design guidelines for realistically sized studies that, if the simulation model is correct, will provide the same information as the large *in silico* study, while exposing the patients to a limited number of experiments.

3.1 Study Design

The *in silico* study included seven T1D virtual patients [1], that each underwent 115 cross-over study days. Model equations and subject specific model parameters are listed in Section 1. At each study day, the IIR was constant at either 1, 2, 3, 4, or 5 times the basal IIR and the glucose infusion rate controlled every five minutes as described previously in Section 2.2.2 to maintain a glucose clamp of 5 mmol/L. After 60 minutes SS run-in period, a glucagon bolus was administered and simulation continued till 5 hours after the bolus. We simulated the effect of the following glucagon boluses: 1 μg, 2.5 μg, 5 μg, 10 μg, 25 μg, 50 μg, 75 μg, 100 μg, 125 μg, 175 μg, 200 μg, 300 μg, 400 μg, 500 μg, 750 μg, 1 mg, 1.5 mg, 2 mg, 3 mg, 4 mg, 5 mg, 7.5 mg, and 10 mg.

3.2 Results and Discussion

The EGP AUCs over 60 minutes (AUC_{60}) were calculated as described in Section 2.2.3. The average EGP AUC_{60} for each dose stratified by IIR were calculated and plotted in Figure 12. The response to glucagon doses below approximately 25 μg are very similar independent of IIR. However, with increasing glucagon doses the curves for each IIR separate. The higher the IIR, the less response to a glucagon bolus. Small increases in glucagon dose during low IIR increase the response significantly although it seems to saturate for some glucagon dose.
The results in Figure 12 represent classical dose-response curves and can be described mathematically by the Michaelis-Menten equation:

$$EGPAUC_{60min} = R_{max} \cdot \frac{Dose}{ED_{50} + Dose} \tag{24}$$

R_{max} is the maximum response and ED_{50} is the dose yielding the half-maximum response. The fitted R_{max} and ED_{50} for each IIR are summarized in Table 8. The ED_{50} does not seem to depend on the insulin level. On the contrary, R_{max} is highly dependent on the insulin level according to Table 8. This observation is expected, as the model used for simulations describes how insulin modulates the maximum achievable EGP response to glucagon, but does not influence the concentration yielding half-maximum response.

Table 8: Fitted parameters for dose-response relationship between glucagon and EGP at multiples of the average basal IIR.

IIR x basal	R_{max}, mg/kg	ED_{50}, mg
1	609	0.220
2	385	0.226
3	183	0.244
4	96	0.256
5	59	0.237

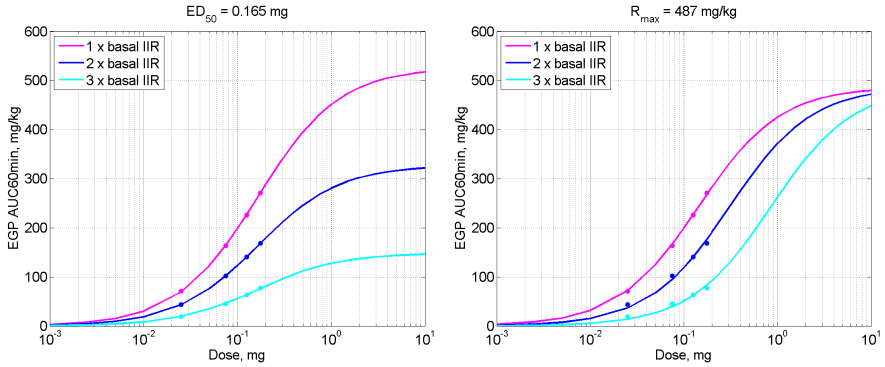

(a) ED_{50} independence of IIR. (b) R_{max} independence of IIR.

Figure 13: Fitted dose response curves when using doses of 25, 75, 125, and 175 μg as in the study by El Youssef *et al.* [2] assuming independence of insulin for either ED_{50} or R_{max}.

3.3 Dose Selection for an *in Vivo* Study

There is speculations to how the ambient insulin level affects the EGP response to glucagon. Two hypothesis are proposed:

- insulin level influences the maximum response to glucagon, R_{max}
- insulin level influences the glucagon dose at which half-maximum response is achieved, ED_{50}

The hypotheses could be examined by carrying out a smaller *in vivo* study. However, the glucagon doses must be carefully chosen to make sure to capture the essential parts of the dose response curve. If all tested doses are below the true ED_{50} both hypotheses would describe the data equally well. This pitfall is illustrated in the following example.

The *in silico* study just described in Section 3.1 was inspired by the results presented in Figure 9 in Section 2.3.4. Assuming the *in vivo* study was carried out again with the same glucagon doses of 25, 75, 125, and 175 μg at one to three times the basal IIR, would one be able to decide which parameter in equation (24) insulin affects?
To answer this question, we simulated the small study and fitted the parameters of (24) twice; first assuming ED_{50} was constant across insulin levels and then assuming R_{max} was constant across insulin levels. The results are presented in Figure 13. Because the four doses are within a narrow dose range and all doses are below the simulated "true" ED_{50}, both hypotheses fit the simulated data equally well. Although the case with equal ED_{50} represents the simulated "truth", the commonly identified ED_{50} is much lower than the parameter value presented in Table 8.

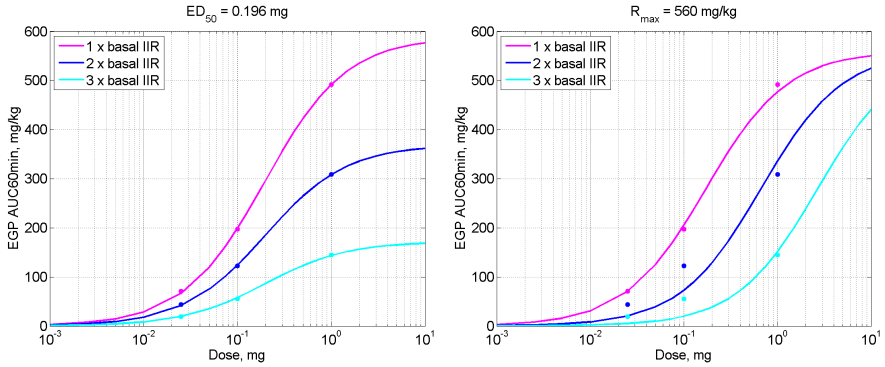

(a) ED_{50} independence of IIR. (b) R_{max} independence of IIR.

Figure 14: Fitted dose response curves when using SC glucagon doses of 25, 100, and 1000 μg assuming independence of insulin for either ED_{50} or R_{max}.

If the glucagon doses had been distributed across a larger dose range encompassing the "true" ED_{50}, would it then be possible to determine how insulin affects EGP? Realistically, one can not administer more than 1 mg glucagon as a SC bolus injection which causes some limitations to the maximum possible dose range in an *in vivo* study. We simulated a small realistic study with three SC glucagon boluses of 25 μg, 100 μg, and 1 mg at one to three times the basal IIR. We then fitted (24) assuming either ED_{50} or R_{max} constant and independent of the ambient insulin level. Figure 14 presents the results using the model analyzed in Section 3.2 where ED_{50} is constant and independent of the ambient insulin level. The graphs visualize a clear difference in the fitness of the two hypotheses making one more plausible than the other; that ED_{50} does not depend on ambient insulin levels, but that R_{max} does. Moreover, the identified common ED_{50} is similar although a bit lower than the values listed in Table 8.

If this study was to be carried out in real life, biological variation between subjects might be dominating making it difficult to determine which hypothesis to accept and which to reject. Instead of relying on the inter-subject variation being low, one could fit (24) to data from individual subjects and hopefully reach the same conclusion in all subjects. The individually confirmed hypothesis could then be transferred to the population mean.

4 Pearls & Pitfalls

This section focuses on the *DOs* and *DON'Ts* when conducting clinical studies of the glucoregulatory system with focus on experiments involving glucagon. The points will be exemplified through simulations and references to literature. We hope that this section serves as an inspiration to researchers who are planning *in vivo* studies of the glucoregulatory system.

4.1 Glucose Clamps

The blood glucose clamp is a procedure used to maintain the same glucose level throughout an experiment either hypoglycaemic (below normal), euglycaemic (normal), or hyperglycaemic (above normal). The purpose of clamping the blood glucose is to eliminate the influence of varying glucose levels during an experiment where glucose is believed to affect the investigated mechanism. As an example, the glucose clamp procedure could be used during a gastric emptying study to eliminate the negative feedback mechanism between blood glucose concentration and gastric emptying rate [10].
The glucose clamp can be controlled using intravenous (IV) infusions of insulin and glucose. Somatostatin may be infused to inhibit endogenous production of hormones like insulin and glucagon in healthy subjects. The glucose regulating hormones are then clamped at continuous rates and as a minimum clamped at the basal rates to substitute for baseline concentrations. Somatostatin may not be necessary in clamp studies when investigating effects of exogenous supraphysiological glucagon doses in patients with type 1 diabetes having no endogenous insulin production.

4.1.1 Glucose Level and Glucose Infusion

An *in vivo* study by Hinshaw *et al.* points to that the glucose level does not influence the effect of glucagon [11]. However, Cherrington advocates there is an inhibitory effect of hyperglycemia on EGP [12]. Therefore, we recommend that the blood glucose concentration is kept close to a set point throughout a clamp experiment involving glucagon to minimize potential influence of the blood glucose concentration on EGP.
The simplest and fastest way to control the glucose level during a clamp is through IV glucose infusion. The glucose infusion can be controlled automatically using various controllers based on PID or Model Predictive Control (MPC). In Section 2.3.5 we demonstrated that a simple PID controller was sufficient to maintain the blood glucose close to a predefined set point while administering glucagon. Moreover, a simple PID controller is easy to implement and may assist investigators in keeping the blood glucose close to the predefined set point level. This is however only possible in cases when the insulin and glucose infusions are sufficiently high to allow for the glucose infusion to be reduced corresponding to the EGP contribution from the glucagon bolus.

4.1.2 Insulin Level and Insulin Infusion

Glucose clamps are not recommended to be controlled by IV insulin infusion although it occurs. Studies have showed that high insulin levels during euglycaemia suppress the

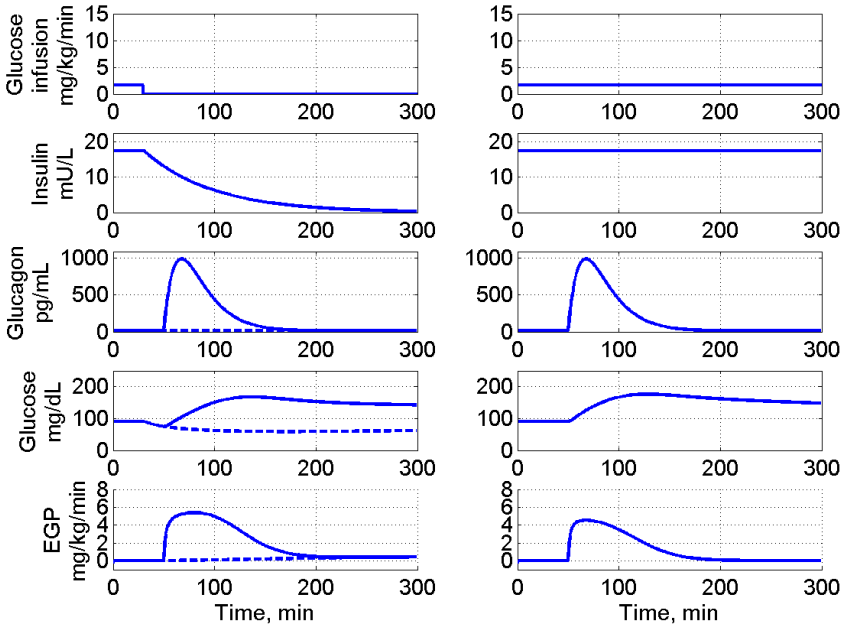

Figure 15: *In silico* demonstration of the dynamics when stopping or continuing IV insulin and glucose infusion during a clamp study in subject 4. Blood glucose was clamped at 5 mmol/L by twice the basal IIR and constant glucose infusion. After 30 minutes SS, glucose and insulin infusions were stopped (left column) and 20 minutes after either no bolus (dashed line) or a 0.5 mg SC glucagon bolus (solid line) was administered. In a different scenario, the insulin and glucose infusions continued throughout the study and a 0.5 mg SC glucagon bolus was administered (right column).

effect of glucagon on EGP [2, 13]. In Section 2 we verified that our simulation model achieved similar results as obtained *in vivo* by El Youssef *et al.* [2]. Should the insulin infusion then be kept constant throughout a clamp experiment? Yes. In the following we demonstrate *in silico* how much insulin levels influence the response to glucagon.

The first *in silico* study design is inspired by Blauw *et al.* [14] to demonstrate that it is difficult to interpret the glucose response to glucagon when too many dynamics influence the response. This situation is illustrated in Figure 15 by simulations and explained in the caption. When insulin and glucose infusions are stopped during a clamp procedure, the immediate response is a drop in glucose levels both due to the lack of glucose infusion and because the effect of insulin persists after the infusion is stopped. Although the glucose responses to glucagon in Figure 15 look fairly similar, more EGP is produced when the infusions are stopped as measured by the AUC. The increased EGP is hiding the drop in glucose that would have been seen if no glucagon bolus was

administered. Even when no glucagon bolus is administered the EGP increases slightly after infusion stop of insulin and glucose because of the fading insulin level.
It should be noted, that the insulin clearance parameters were estimated from data following SC insulin administration rather than IV administration, which could underestimate the actual clearance since it is limited by the slow and variable SC absorption.

The second *in silico* study design explores what happens if one uses insulin to control a glucose clamp rather than glucose. The blood glucose of a patient undergoing a glucose clamp responds immediately to the changes in the glucose infusion whereas the effect of insulin is delayed. An example to illustrate the delayed effect of insulin is demonstrated in Figure 16 by simulations and explained in the caption. Although the same glucagon bolus of 0.5 mg was given at the same insulin concentration, the responses were different - the larger the prior SC insulin bolus, the smaller response to glucagon. However, not all virtual patients seem to have as pronounced delayed response to insulin as in this example. The size of the delay highly depends on the parameter k_{a3} in the PD model which represents the rate constant of remote insulin action on EGP, see Table 4 in Section 1.4.

The simulated examples show that the insulin level highly influences the EGP response to glucagon and the effect of insulin can be delayed.

4.2 Dynamics in Data

A model can only be expected to describe dynamics present in the data used for model development and parameter estimation, if data is sampled sufficiently. To correctly estimate Tmax after a bolus administration in a PK model, data must be sampled densely around Tmax. If Tmax of a compound is expected to be 50 minutes, and no samples are collected the first two hours after dose administration, it is practically impossible to determine Tmax without inferring prior knowledge. More importantly, if Tmax is very short the exact notation of the dosing time is absolutely necessary in order to fit a meaningful PK model to data.

Furthermore, factors influencing the model parameters can not be included in the description of the parameters if the factors do not vary in the training dataset. As an example, exercise and stress are long known to alter the insulin sensitivity, and recently Ranjan *et al.* found that diet might influence the response to glucagon [15]. None of these factors are accounted for in the glucose PD model used for simulations throughout this report [1]. Moreover, the model does not include a feedback mechanism of the glucose levels to the endogenous production of insulin and glucagon.

4.2.1 Identifying Steady State

As described, the final fitted model is limited by the data used for estimating the model parameters. Thus identifying the correct steady state can be difficult if the data do not contain much information thereof. Figure 17 illustrates that the PD model described in [1] does not estimate the correct steady state. Initializing patient 7 at euglycaemia with

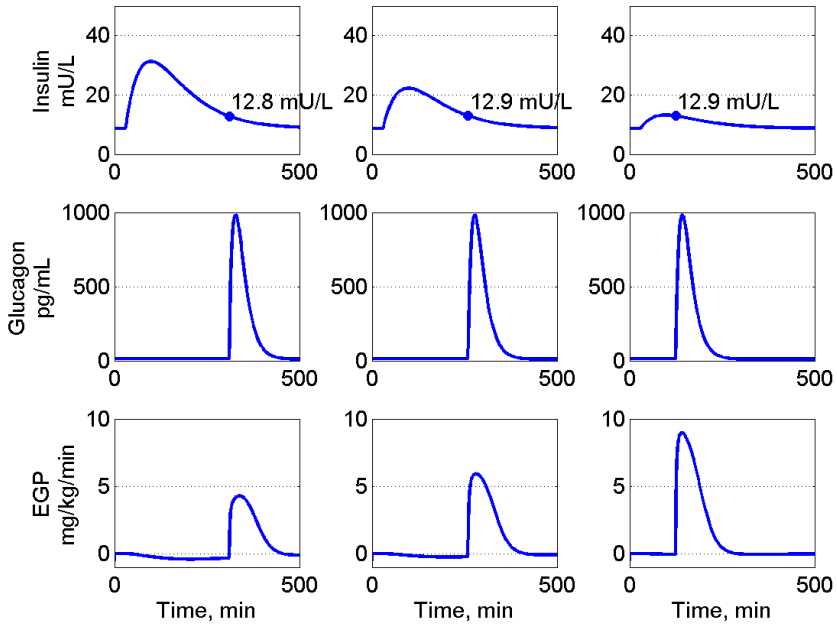

Figure 16: *In silico* demonstration of the delayed insulin effect on EGP. Blood glucose was clamped at 5 mmol/L by basal IIR and controlled via IV glucose infusion every 5 minutes using the PID controller explained in Section 2.2.2. After 30 minutes steady state, subject 4 received a SC insulin bolus of either 5 U (left), 3 U (middle) or 1 U (right). When the insulin concentration dropped below 13 mU/L a SC glucagon bolus of 0.5 mg was administered. The EGP responses are displayed in the bottom row; the 120 minutes AUCs are 323, 429, and 612 mg/kg, respectively.

baseline levels of insulin and glucagon as in Figure 17a, one would expect the glucose level to stay constant or at least approach a level similar to either of the observed initial values. However, the glucose concentration drops to a level below 50 mg/dL. The reason for this behaviour is explained in the data used for estimating the model parameters of patient 7 [1,16], see Figure 17b. The data contains very little information about the insulin, glucagon and glucose levels before the system is disturbed with an insulin bolus. On the contrary, it appears that a SS is achieved towards the end of the experiment when the glucose concentration is around 50 mg/dL and both glucagon and insulin have returned to their baseline levels. This phenomenon explains why the model assumes glucose SS lower than one would expect at baseline levels of insulin and glucagon.

4.2.2 Repeated Glucagon Boluses

When conducting experiments *in vivo* one naturally wishes to maximize the information from those experiments. Clinical studies are often set up to investigate multiple glucagon doses during each trial day [2, 14]. However, depending on the size of the glucagon bolus, it can take several hours before all administered drug is cleared from the system and plasma concentration has returned to baseline. As evident in Figure 17b, plasma glucagon has only just returned to baseline four hours after a SC bolus of 300 μg glucagon. Be reminded of Figure 10 in Section 2 where the continuous increase in glucose concentration is due to residual glucagon from the previous dose. One must allow sufficient time in-between experiments and perhaps lower ones expectations to what is practically possible to avoid carry-over effects from previous doses, rather than rushing too many experiments in short time.

4.2.3 The Glucagon Evanescence Effect

The glucagon evanescence effect is well known and documented since the early 1980s [11, 17, 18]. As implied in the name, the effect of glucagon tends to fade away over time. This trend is observed during clamp studies with constant insulin and glucagon levels where the EGP tends to return to baseline after approximately two hours although the glucagon level is still significantly elevated above the baseline level [11,18]. Mechanisms to explain this phenomenon could be degradation/aggregation of infused glucagon, hyperglycemia, intra-hepatic negative feedback mechanism or simply glycogen depletion.
As the evanescence effect is observed even during clamped euglycaemia, hyperglycemia can not solemnly explain the vanishing effect of glucagon [11].
Glycogen depletion seems like an easy explanation. However, the amount of infused glucagon during the study by Hinshaw *et al.* [11] was 0.54 μg/kg over three hours during the highest glucagon infusion rate. A study by Castle *et al.* [19] found that repeated boluses of 2 μg/kg did not deplete the liver even after an overnight fast. Therefore, it does not seem likely that the evanescence effect observed during clamp studies of glucagon is due to depletion of the glycogen stores in the liver.
In vitro data suggest that the glucagon evanescence effect is due to desensitization of the receptor regulated by cyclic AMP [20]. The reduced responsiveness to glucagon was fully expressed after 2 hours which fits well with *in vivo* data [11, 18]. Hinshaw *et al.* [11] proposed a mathematical expression to capture the waning effect of glucagon. However, it is unclear for how long this evanescence effect persists and if a sudden increase in the glucagon infusion can overrule the evanescence phenomenon. More studies of the glucagon evanescence effect are needed to fully understand the underlying mechanisms and how the effect should be accounted for in a glucoregulatory model including glucagon.

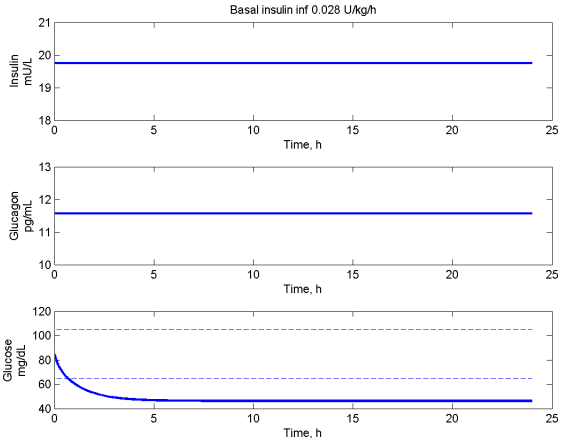

(a) Simulation of subject 7's modelled SS. Insulin and glucagon are at baseline levels, and glucose concentration initiated at euglycaemia.

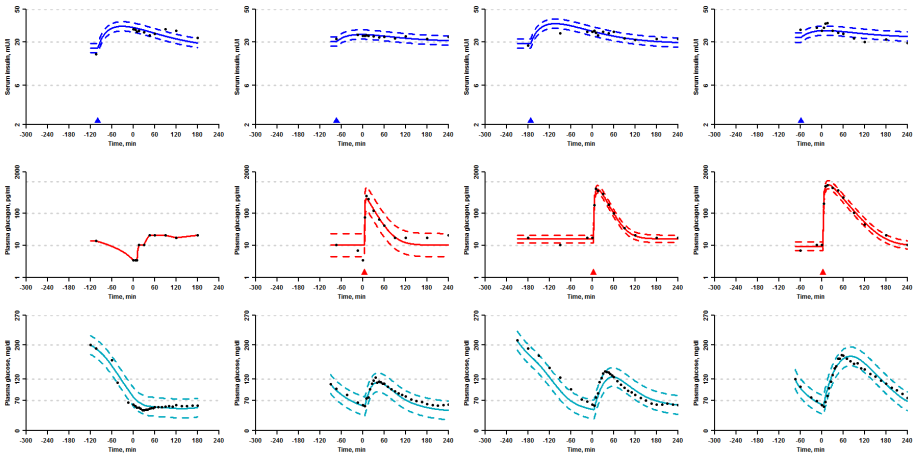

(b) Raw data and PK/PD model fits in subject 7: insulin PK (top), glucagon PK (middle), glucose PD (bottom). Increasing glucagon boluses left to right: 0, 100, 200, 300 μg. Triangles indicate time of insulin bolus (blue) and glucagon bolus (red). Please see [1] for further study details.

Figure 17: Comparison of modelled SS and data used for model building.

4.3 Summary

The learnings of the previous sections can be summed up in the following statements that should aid in the design of clinical studies:

- The glucose level during hypo- or euglycaemia does not influence the glucose response to glucagon.
- Theoretically, a simple PID controller can control the needed glucose infusion to maintain constant glucose levels when the insulin infusion is sufficiently high.
- The insulin infusion should be constant throughout the study duration.
- Nominal sampling times must be chosen carefully and actual sampling times noted meticulously.
- A model can only be expected to account for dynamics present in the dataset used for model building and parameter estimation.
- Less is more. Avoid multiple dynamics simultaneously by allowing enough time between disturbances of the glucoregulatory system.
- The effect of glucagon wanes over time despite constant infusion.
- Glucagon doses should be distributed across a wide range encompassing the true half maximum response in order to correctly identify the dose-response relationship.

References

[1] S. L. Wendt, A. Ranjan, J. K. Møller, S. Schmidt, C. B. Knudsen, J. J. Holst, S. Madsbad, H. Madsen, K. Nørgaard, and J. B. Jørgensen, "Cross-validation of a glucose-insulin-glucagon pharmacodynamics model for simulation using data from patients with type 1 diabetes," *Journal of Diabetes Science & Technology*, 2017.

[2] J. El Youssef, J. R. Castle, P. A. Bakhtiani, A. Haidar, D. L. Branigan, M. Breen, and W. K. Ward, "Quantification of the glycemic response to microdoses of subcutaneous glucagon at varying insulin levels," *Diabetes Care*, vol. 37, no. 11, pp. 3054–3060, 2014.

[3] A. Haidar, C. Duval, L. Legault, and R. Rabasa-Lhoret, "Pharmacokinetics of insulin aspart and glucagon in type 1 diabetes during closed-loop operation," *Journal of diabetes science and technology*, vol. 7, no. 6, pp. 1507–1512, 2013.

[4] S. L. Wendt, J. K. Møller, C. B. Knudsen, H. Madsen, A. Haidar, and J. B. Jørgensen, "Pk/pd modelling of glucose-insulin-glucagon dynamics in healthy dogs after a subcutaneous bolus administration of native glucagon or a novel glucagon analogue," Technical University of Denmark, Tech. Rep. 2, April 2016.

[5] S. L. Wendt, J. K. Møller, A. Haidar, C. B. Knudsen, H. Madsen, and J. B. Jørgensen, "Modelling of glucose-insulin-glucagon pharmacodynamics in man," in *Proceedings of the 38th Annual International Conference of the IEEE Engineering in Medicine and Biology Society*. IEEE EMBS, 2016.

[6] F. Q. Nuttall, A. Ngo, and M. C. Gannon, "Regulation of hepatic glucose production and the role of gluconeogenesis in humans: is the rate of gluconeogenesis constant?" *Diabetes/Metabolism Research and Reviews*, vol. 24, no. 6, pp. 438–458, 2008.

[7] R. Hovorka, F. Shojaee-Moradie, P. V. Carroll, L. J. Chassin, I. J. Gowrie, N. C. Jackson, R. S. Tudor, A. M. Umpleby, and R. H. Jones, "Partitioning glucose distribution/transport, disposal, and endogenous production during IVGTT," *American Journal of Physiology-Endocrinology and Metabolism*, vol. 282, no. 5, pp. E992–E1007, 2002.

[8] R. Hovorka, V. Canonico, L. J. Chassin, U. Haueter, M. Massi-Benedetti, M. O. Federici, T. R. Pieber, H. C. Schaller, L. Schaupp, T. Vering, and M. E. Wilinska, "Nonlinear model predictive control of glucose concentration in subjects with type 1 diabetes," *Physiological measurement*, vol. 25, no. 4, pp. 905–920, 2004.

[9] N. J. W. Albrechtsen, B. Hartmann, S. Veedfald, J. A. Windeløv, A. Plamboeck, K. N. Bojsen-Møller, T. Idorn, B. Feldt-Rasmussen, F. K. Knop, T. Vilsbøll, S. Madsbad, C. F. Deacon, and J. J. Holst, "Hyperglucagonaemia analysed by glucagon sandwich elisa: nonspecific interference or truly elevated levels?" *Diabetologia*, vol. 57, no. 9, pp. 1919–1926, 2014.

[10] M. Horowitz, D. O'Donovan, K. L. Jones, C. Feinle, C. K. Rayner, and S. M., "Gastric emptying in diabetes: clinical significance and treatment," *Diabetic Medicine*, vol. 19, no. 3, pp. 177–194, 2002.

[11] L. Hinshaw, A. Mallad, C. D. Man, R. Basu, C. Cobelli, R. E. Carter, Y. C. Kudva, and A. Basu, "Glucagon sensitivity and clearance in type 1 diabetes: insights from in vivo and in silico experiments," *American Journal of Physiology, Endocrinology and Metabolism*, vol. 309, no. 5, pp. E474–E486, 2015.

[12] A. D. Cherrington, "Control of glucose production in vivo by insulin and glucagon," in *Comprehensive Physiology 2011, Supplement 21: Handbook of Physiology, The Endocrine System, The Endocrine Pancreas and Regulation of Metabolism*, First published in print 2001, pp. 759–785.

[13] K. E. Steiner, P. E. Williams, W. W. Lacy, and A. D. Cherrington, "Effects of insulin on glucagon-stimulated glucose production in the conscious dog," *Metabolism*, vol. 39, no. 12, pp. 1325–1333, 1990.

[14] H. Blauw, I. Wendl, J. H. DeVries, T. Heise, and T. Jax, "Pharmacokinetics and pharmacodynamics of various glucagon dosages at different blood glucose levels," *Diabetes, Obesity and Metabolism*, vol. 18, no. 1, pp. 34–39, 2016.

[15] A. Ranjan, S. Schmidt, C. Damm-Frydenberg, I. Steineck, T. R. Clausen, J. J. Holst, S. Madsbad, and K. Nørgaard, "Low carbohydrate diet impairs the effect of glucagon in the treatment of insulin-induced mild hypoglycemia: A randomized cross-over study," *Diabetes Care*, vol. Epub ahead of print, 2016.

[16] A. Ranjan, S. Schmidt, S. Madsbad, J. J. Holst, and K. Nørgaard, "Effects of subcutaneous, low-dose glucagon on insulin-induced mild hypoglycaemia in patients with insulin pump treated type 1 diabetes." *Diabetes, Obesity and Metabolism*, vol. 18, no. 4, pp. 410–418, 2016.

[17] A. Cherrington, P. Williams, G. Shulman, and W. Lacy, "Differential time course of glucagon's effect on glycogenolysis and gluconeogenesis in the conscious dog," *Diabetes*, vol. 30, no. 3, pp. 180–187, 1981.

[18] M. Wada, C. C. Connolly, C. Tarumi, D. W. Neal, and A. D. Cherrington, "Hepatic denervation does not significantly change the response of the liver to glucagon in conscious dogs," *American Journal of Physiology - Endocrinology and Metabolism*, vol. 268, no. 2, pp. E194–E203, 1995.

[19] J. R. Castle, J. El Youssef, P. A. Bakhtiani, Y. Cai, J. M. Stobbe, D. Branigan, K. Ramsey, P. Jacobs, R. Reddy, M. Woods, and W. K. Ward, "Effect of repeated glucagon doses on hepatic glycogen in type 1 diabetes: Implications for a bihormonal closed-loop system," *Diabetes care*, vol. 38, no. 11, pp. 2115–2119, 2015.

[20] F. R. DeRubertis and P. Craven, "Reduced sensitivity of the hepatic adenylate cyclase-cyclic amp system to glucagon during sustained hormonal stimulation," *Journal of Clinical Investigation*, vol. 57, no. 2, pp. 435–443, 1976.